International Journal of Engineering Trends and Technology
ISSN: 2231–5381 / https://doi.org/10.14445/22315381/IJETT-V72I2P126

Volume 72 Issue 2, 254-266, February 2024

Original Article

Dimensional Synthesis of Four-Bar Mechanisms for the Generation of Rectilinear Motion Through Analytical and Graphical Programming and Optimization of the Straight Trajectory of the Coupling Point

BODIE NGUEMIENGO Abdel Axis[1,2*], NGAYIHI ABBE Claude Valery[1,2], KOM Charles Hubert[1,2]

[1]*Energy, Materials, Modeling and Methods Research Laboratory (E3M), Université de Douala, Cameroun.*
[2]*Higher National Polytechnic School of Douala, Université de Douala, Cameroun.*

[*]*Corresponding Author : bodieabdel@gmail.com*

Received: 12 June 2023 Revised: 28 July 2023 Accepted: 06 January 2024 Published: 03 February 2024

Abstract - *This article deals with the dimensional synthesis of four-bar mechanisms for the generation of rectilinear motion through analytical and graphical programming and optimization of the straight trajectory of the coupling point. The work carried out to date on synthesizing four-bar mechanisms enables the objective function to be optimized, but the trajectory of the coupling point is always curvilinear when the mechanism is in motion. This work presents a method for generating a rectilinear motion of the coupling point by finding the interval in which the crank input angle must vary to obtain reciprocating rectilinear motion. The advantage of this method is that it is precise, given that it considers the global programming of all the blocks that define the various equations and relationships between angles and distances existing in the four-bar mechanism. Convergence is rapid, as we have verified with five precision points, which verify the equation of a straight line, with the coupling point whose coordinates verify the equations of a straight line to obtain rectilinear motion. Analytical and graphical programming allows us to treat the problem by subdividing it into function program blocks and highlighting their interactions. Trajectory optimization is achieved by forcing the coupling point to pass only on a straight line, thus obtaining rectilinear motion instead of a curvilinear curve, as encountered in the literature.*

Keywords - *Analytical synthesis, Four-bar mechanisms, Graphical programming, Rectilinear motion generation, Straight path optimization.*

1. Introduction

The synthesis of the trajectory of a four-bar mechanism has been actively studied over the last fifty years. A large number of studies have been carried out using a variety of methods. These include analytical programming [1,2], continuation [3], nonlinear objective programming [4,5], exact gradient [6], coupler-angle function curve [7], and curve curvature methods [8]. The problem of trajectory synthesis of a four-bar mechanism is to generate a mechanism whose coupling point can trace the desired trajectory or target points. There is no analytical solution to the general problem of synthesizing a four-bar mechanism for more than five precision points. Various numerical methods can solve this type of problem. For example, it can be seen as optimizing a mechanism to minimize an objective function. A very important task in a design process is to know how to manufacture a mechanism that will satisfy the desired motion characteristics of an element, i.e., a mechanism in which a part will certainly execute the desired motion.

There are three common requirements in the kinematic synthesis of mechanisms: trajectory generation, function generation, and motion generation. In dimensional synthesis, there are two approaches: precision point synthesis and approximate or optimal synthesis [9].

Precision point synthesis implies that the point at the end of a mechanism (usually a coupler in a four-bar linkage) passes through a number of desired points but without the possibility of controlling a structural error on a path out of these points. The synthesis of precision points is limited by the number of points, which must be equal to the number of independent parameters defined by the mechanism. The maximum number of points for a four-bar link is nine. If the number of equations generated by the number of precision points is less than the number of projected equations, the mechanism can perform point synthesis. As the number of exact points increases, the problem of exact point synthesis becomes highly nonlinear and extremely difficult to solve.

In most cases, the mechanism obtained by this type of synthesis is very difficult to solve. In most cases, this type of synthesis is useless. There is no mechanism because the dimensions of the mechanism's elements are disproportionately large, or the solutions obtained are in the form of complex numbers.

The maximum number of precision points on the coupler path of a four-bar mechanism is five in coordinated motion and nine in uncoordinated motion. It can be seen that mechanism synthesis using precision point methods is limited by the number of points given, and increasing precision points to more than nine is virtually impossible. Optimal mechanism synthesis is, in fact, repeated analysis of a randomly determined mechanism and the search for the best possible mechanism to meet technological requirements, and is most often used in dimensional synthesis, which involves determining the elements of a given mechanism (bar lengths, angles, coordinates, etc.) needed to create the mechanism in the desired direction.The optimization algorithm contains the objective function defined by the synthesis problem and represents a set of mathematical relationships; it must be chosen so that the conditions perform the desired tasks presented in a well-defined mathematical form. The objective function is assigned a numerical value for each solution.

Ideally, it should result in a global minimum, corresponding to the algorithm's lowest value and the best possible mechanism that should execute a technological procedure, but this is difficult to achieve due to very complex problems.The objective function can contain various restrictions, such as restricting the ratio of limb lengths, preventing negative limb lengths, negative limb lengths, restrictions on transmission angles, and so on. For this purpose, so-called penalty functions are introduced, which considerably increase the value of the objective function when the values mentioned point in an undesirable direction. The penalty functions included in the objective function during mechanism synthesis are also called equalization functions, as they transform the restricted optimization problem into an unrestricted one [9].

It has been pointed out that the synthesized solution may be unusable due to circuit or control faults or be unable to move from one coupling point to another.Although a synthesized solution may be found at the plotted points, there is no guarantee as to the behavior of the connection between these points. A circuit fault occurs when the link is unable to move in a region between these plotted points, i.e., between the coupling points [10].From the work carried out to date, it appears essential to optimize the objective function for dimensional synthesis and trajectory optimization of a bar mechanism, which in the vast majority of cases requires the hybridization of genetic algorithms or nonlinear programming.

Similarly, six- and eight-bar mechanisms are the most commonly used for rectilinear motion generation applications, as four-bar mechanisms have rectilinear motion on a portion of the trajectory. The latter can be observed in the results of previous work [9,10].

This work proposes an alternative method or approach in which analytical and graphical programming is used to define, firstly, all the existing relationships and equations between bar lengths and angles and, secondly, to optimize the straight trajectory of 4-bar mechanisms and find which intervals of the input angle rectilinear motion is observed. The shortcomings or limitations of this method are that, for each type of bar mechanism, the existing equations and relationships between the bar lengths and the various angles between the bars must be determined manually before entering the data and expressions into MATLAB.

Then, the function blocks and the existing interactions between them must be precisely defined - indeed, the slightest error in an equation or function block will distort the results. In this case, the objective function is not optimized; rather, the straight trajectory of the coupling point is optimized, referred to as trajectory synthesis. This work aims to carry out a dimensional synthesis of four-bar mechanisms for generating rectilinear motion by optimizing the straight trajectory of the coupling point and finding the range in which it can be obtained. Given that no four-bar mechanism performs a perfectly rectilinear motion at the output of the coupler, analytical programming will be used to impose the equation of the straight line that the coordinates of the coupling point must verify, and then with the help of graphical programming, find the interval of the input angle in which the mechanism's motion is rectilinear.

A 2D sketch produced by SolidWorks® or GeoGebra is used to check whether the synthesized mechanism is flawed. The latter is also useful for examining the distance between the precision point and the synthesized coupling point obtained from the synthesized geometric parameters and position equations; finally, the trajectory obtained is compared with that obtained in the most recent work on dimensional synthesis of 4-bar mechanisms [9,10].

2. Materials and Methods

MATLAB 2018a with SIMULINK will be used for programming and analytical synthesis of the mechanism; ARDUINO 2.1.0 for programming crank motion control as a function of input angle variation; GeoGebra for displaying the results of mechanism point trajectories after optimization of the straight trajectory of the coupling point; SOLIDWORS 2022 for simulation of mechanism operation after dimensional synthesis and trajectory optimization, all on an HP 15 Pavilion notebook; Core i5 2.4 GHz processor; 12 GB RAM; 2 GB graphics card and 1 TB hard disk.

2.1. Parameters, Expressions, and Equations Relating Bar Lengths and Angles in the Mechanism

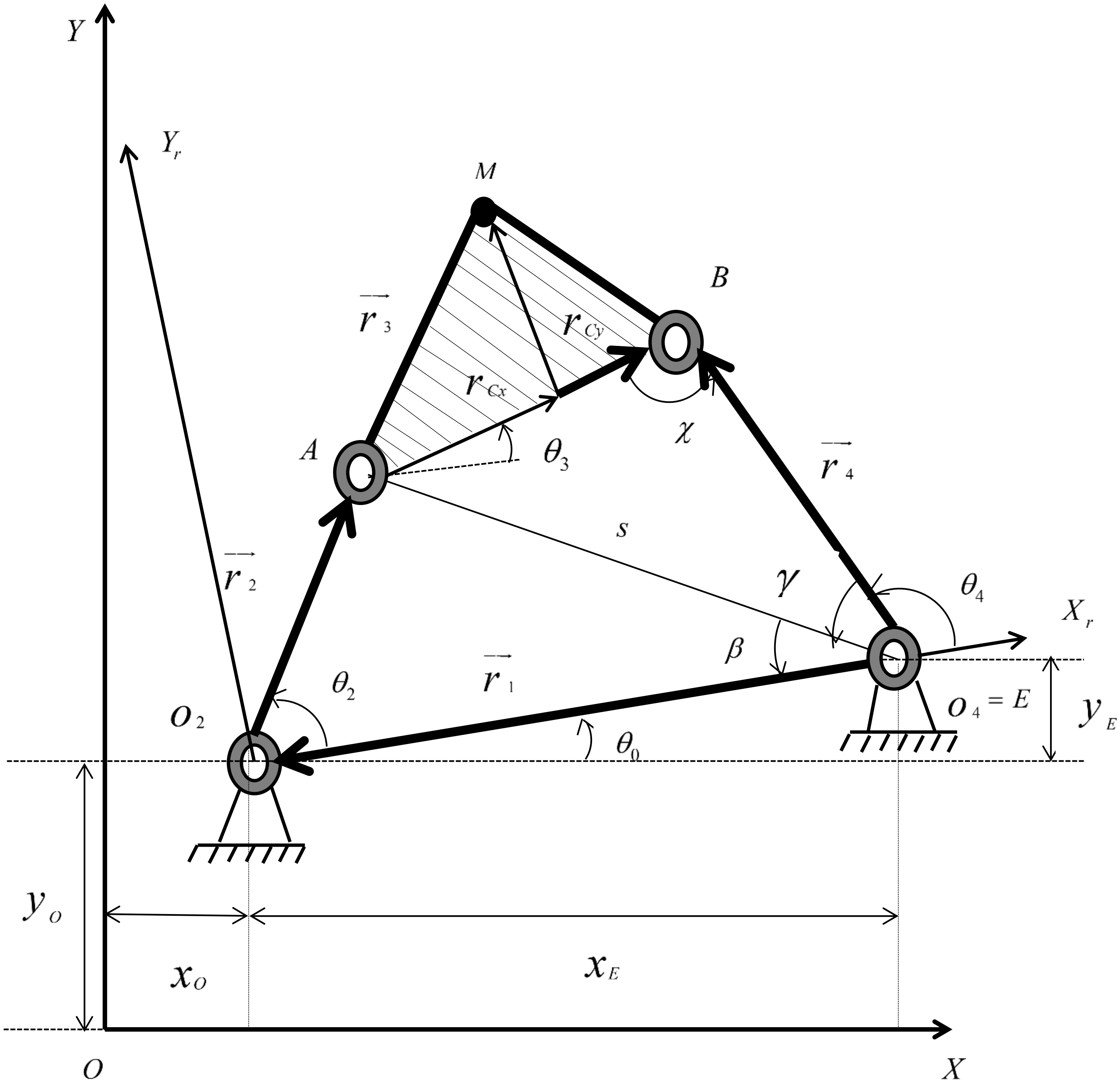

Fig. 1 Global representation of the for-bar mechanism with its dimensions

Analytical programming will use all the data and expressions in this section to define everything according to the input parameters.

2.1.1. Design Parameters

At least nine design parameters for trajectory generation with prescribed timing, r_1, r_2, r_3, r_4, r_{cx}, r_{cy}, x_0, y_0, and θ_0, to be optimized. In addition to the nine design parameters, there are input angles θ_2, θ_2^i (i=1-N) corresponding to precision points and coupling points that must be optimized for trajectory generation.

The vector of design variables X is given as follows:

$$X = \left[r_1, r_2, r_3, r_4, r_{cx}, r_{cy}, x_o, y_o, \theta_0, \theta_2^1, \theta_2^2 ... \theta_2^N \right] \quad (1)$$

N is the number of precision points for optimizing the objective function.

2.1.2. Main Expressions for Analytical Programming

Expression for s in Frame ($O_2X_rY_r$)

Expression of s, the variable defining the distance between the movable crank vertex and point E (O_4) of the frame in the ($O_2X_rY_r$) reference frame.

$$s = \sqrt{r_1^2 - 2\cos(\theta_2) r_1 r_2 + r_2^2} \tag{2}$$

Expression of χ , angle formed between coupler and balance wheel

$$\chi = acos\left(r_3 r_4 \left(-\frac{r_1^2}{2} + \cos(\theta_2) r_1 r_2 - \frac{r_2^2}{2} + \frac{r_3^2}{2} + \frac{r_4^2}{2} \right) \right) \tag{3}$$

From this expression, the expression for s is given, considering the distance between the four bars and the angle of entry between the frame and the crank.

$$s = \sqrt{r_3^2 + r_4^2 - 2r_3^2 r_4^2 \left(-\frac{r_1^2}{2} + \cos(\theta_2) r_1 r_2 - \frac{r_2^2}{2} + \frac{r_3^2}{2} + \frac{r_4^2}{2} \right)} \tag{4}$$

Expression of β, the angle formed between the building and AE

$$\beta = \cos^{-1}\left(\frac{r_1^2 - r_2^2 + r_3^2 + r_4^2 - \sigma_1}{2r_1\sqrt{r_3^2 + r_4^2 - \sigma_1}} \right) \tag{5}$$

With

$$\sigma_1 = 2r_3^2 r_4^2 \left[-\frac{r_1^2}{2} + \cos(\theta_2) r_1 r_2 - \frac{r_2^2}{2} + \frac{r_3^2}{2} + \frac{r_4^2}{2} \right] \tag{6}$$

Expressions of angles θ_3 and θ_4

According to the Freudeinstein equations below

$$r_2 \cos(\theta_2) + r_3 \cos(\theta_3) - r_4 \cos(\theta_4) - r_1 = 0 \tag{7}$$

$$r_2 \sin(\theta_2) + r_3 \sin(\theta_3) - r_4 \sin(\theta_4) = 0 \tag{8}$$

$$k_1 \cos(\theta_4) - k_2 \cos(\theta_2) + k_3 = \cos(\theta_2 - \theta_4) \tag{9}$$

$$k_1 \cos(\theta_3) + k_4 \cos(\theta_2) + k_5 = \cos(\theta_2 - \theta_3) \tag{10}$$

$$k_1 = \frac{r_1}{r_2} \tag{11}$$

$$k_2 = \frac{r_1}{r_4} \tag{12}$$

$$k_3 = \frac{r_1^2 + r_2^2 - r_3^2 + r_4^2}{2r_2 r_4} \tag{13}$$

$$k_4 = \frac{r_1}{r_3} \tag{14}$$

$$k_5 = -\frac{r_1^2 + r_2^2 + r_3^2 - r_4^2}{2r_2 r_3} \tag{15}$$

The expressions are

$$\theta_3 = 2\tan^{-1}\left(\frac{-V \pm \sqrt{V^2 - 4JW}}{2J} \right) \tag{16}$$

$$\theta_4 = 2\tan^{-1}\left(\frac{-H \pm \sqrt{H^2 - 4GI}}{2G} \right) \tag{17}$$

With,

$$G = \cos(\theta_2) - \frac{r_1}{r_2} + \frac{r_1^2 + r_2^2 - r_3^2 + r_4^2}{2r_2 r_4} - \frac{r_1 \cos(\theta_2)}{r_4} \tag{18}$$

$$H = -2\sin(\theta_2) \tag{19}$$

$$I = \frac{r_1}{r_2} - \cos(\theta_2)\left(\frac{r_1}{r_4} + 1 \right) + \frac{r_1^2 + r_2^2 - r_3^2 + r_4^2}{2r_2 r_4} \tag{20}$$

$$J = \cos(\theta_2) - \frac{r_1}{r_2} - \frac{r_1^2 + r_2^2 + r_3^2 - r_4^2}{2r_2 r_3} + \frac{r_1 \cos(\theta_2)}{r_3} \tag{21}$$

$$V = -2\sin(\theta_2) \tag{22}$$

$$W = \cos(\theta_2)\left(\frac{r_1}{r_3} - 1 \right) + \frac{r_1}{r_2} - \frac{r_1^2 + r_2^2 + r_3^2 - r_4^2}{2r_2 r_3} \tag{23}$$

This gives us

$$\theta_4 = 2\tan^{-1}\left[\frac{2\sin(\theta_2) \pm \sqrt{4\sin(\theta_2)^2 - \left(\frac{r_1}{r_2} - \cos(\theta_2)\left(\frac{r_1}{r_4} + 1 \right) + \frac{\sigma_1}{2r_2 r_4} \right)\left(4\cos(\theta_2) - \frac{4r_1}{r_2} + \frac{2\sigma_1}{r_2 r_4} - \frac{4r_1 \cos(\theta_2)}{r_4} \right)}}{2\cos(\theta_2) - \frac{2r_1}{r_2} + \frac{2\sigma_1}{r_2 r_4} - \frac{2r_1 \cos(\theta_2)}{r_4}} \right]$$

(24)

$$\theta_3 = 2\tan^{-1}\left[\frac{2\sin(\theta_2) \pm \sqrt{4\sin(\theta_2)^2 - \left(\cos(\theta_2)\left(\frac{r_1}{r_3} - 1 \right) + \frac{r_1}{r_2} - \frac{\sigma_1}{2r_2 r_3} \right)\left(4\cos(\theta_2) - \frac{4r_1}{r_2} - \frac{2\sigma_1}{r_2 r_3} + \frac{4r_1 \cos(\theta_2)}{r_3} \right)}}{2\cos(\theta_2) - \frac{2r_1}{r_2} - \frac{\sigma_1}{r_2 r_3} + \frac{2r_1 \cos(\theta_2)}{r_3}} \right]$$

(25)

With $\sigma_1 = r_1^2 + r_2^2 - r_3^2 + r_4^2$

Expression of the angle between the crank and the abscissa axis (horizontal) of the general reference frame (OXY)

$$\varphi = \theta_0 + \theta_2 \tag{26}$$

Expression of the coordinates of point A

$$x_A = x_0 + r_2\cos\left(\theta_0 + \theta_2\right) \quad (27)$$

$$y_A = y_0 + r_2\sin\left(\theta_0 + \theta_2\right) \quad (28)$$

$$A = \begin{pmatrix} x_0 + r_2\cos\left(\theta_0+\theta_2\right) \\ y_0 + r_2\sin\left(\theta_0+\theta_2\right) \end{pmatrix} \quad (29)$$

Expression of s in frame (OXY)

$$E = \begin{pmatrix} x_E \\ y_E \end{pmatrix} = \begin{pmatrix} r_1\cos\theta_0 \\ r_1\sin\left(\sqrt{r_1^{\,2} - (r_1\cos\theta_0)^2}\right) \end{pmatrix} \quad (30)$$

$$s = \sqrt{\left(x_E - r_2\cos\left(\theta_0+\theta_2\right)\right)^2 + \left(y_E - r_2\sin\left(\theta_0+\theta_2\right)\right)^2} \quad (31)$$

Expression of θ

$$\theta = \gamma + \theta_4 \quad (32)$$

$$\theta = r_2\tan\left(\frac{y_E - r_2\sin\left(\theta_0+\theta_2\right)}{x_E - r_2\cos\left(\theta_0+\theta_2\right)}\right) \quad (33)$$

Expression of the angle between s and r_4

$$\gamma = cos^{-1}\left(\frac{\left(x_E - r_2\cos\left(\theta_0+\theta_2\right)\right)^2 + \left(y_E - r_2\sin\left(\theta_0+\theta_2\right)\right)^2 - r_3^{\,2} + r_4^{\,2}}{2r_4\sqrt{\left(x_E - r_2\cos\left(\theta_0+\theta_2\right)\right)^2 + \left(y_E - r_2\sin\left(\theta_0+\theta_2\right)\right)^2}}\right) \quad (34)$$

Expression of B coordinates

$$x_B = x_0 + x_E + r_4\cos\left[t\cos^{-1}\left(\frac{\sigma_2 + \sigma_1 - r_3^{\,2} + r_4^{\,2}}{2r_4\sqrt{\sigma_2+\sigma_1}}\right)\right] - r_2\tan\left[\frac{y_E - r_2\sin\left(\theta_0+\theta_2\right)}{x_E - r_2\cos\left(\theta_0+\theta_2\right)}\right] \quad (35)$$

$$y_B = y_0 + y_E - r_4\sin\left[t\cos^{-1}\left(\frac{\sigma_2 + \sigma_1 - r_3^{\,2} + r_4^{\,2}}{2r_4\sqrt{\sigma_2+\sigma_1}}\right)\right] - r_2\tan\left[\frac{y_E - r_2\sin\left(\theta_0+\theta_2\right)}{x_E - r_2\cos\left(\theta_0+\theta_2\right)}\right] \quad (36)$$

With $\sigma_1 = \left[y_E - r_2\sin(\theta_0+\theta_2)\right]^2$ (37)

$$\sigma_2 = \left[x_E - r_2\cos(\theta_0+\theta_2)\right]^2 \quad (38)$$

B, therefore, has the coordinates.

$$B = \begin{pmatrix} x_0 + x_E + r_4\cos\left(\sigma_1\right) \\ y_0 + y_E - r_4\sin\left(\sigma_1\right) \end{pmatrix} \quad (39)$$

Expression of ψ

$$\psi = -r_2\tan\left[\frac{r_2\sin\left(\theta_0+\theta_2\right) - y_E + r_4\sin\left(\sigma_1\right)}{x_E - r_2\cos\left(\theta_0+\theta_2\right) + r_4\cos\left(\sigma_1\right)}\right] \quad (40)$$

With

$$\sigma_1 = t\cos^{-1}\left(\frac{\sigma_3 + \sigma_2 - r_3^{\,2} + r_4^{\,2}}{2r_4\sqrt{\sigma_3+\sigma_2}}\right) - r_2\tan\left[\frac{y_E - r_2\sin\left(\theta_0+\theta_2\right)}{x_E - r_2\cos\left(\theta_0+\theta_2\right)}\right] \quad (41)$$

$$\sigma_2 = \left[y_E - r_2\sin(\theta_0+\theta_2)\right]^2 \quad (42)$$

$$\sigma_3 = \left[x_E - r_2\cos(\theta_0+\theta_2)\right]^2 \quad (43)$$

Expression of coordinates of point M

$$x_M = x_0 + r_{cy}\cos\left(\frac{\pi}{2} - \sigma_1\right) + \sigma_3 + r_{cx}\cos(\sigma_1) \quad (44)$$

With

$$\sigma_1 = r_2\tan\left[\frac{r_2\sin\left(\theta_0+\theta_2\right) - y_E + r_4\sin\left(\sigma_2\right)}{x_E - \sigma_3 + r_4\cos(\sigma_2)}\right] \quad (45)$$

$$\sigma_2 = t\cos^{-1}\left(\frac{(x_E-\sigma_3)^2 + (y_E - r_2\sin(\theta_0+\theta_2))^2 - r_3^{\,2} + r_4^{\,2}}{2r_4\sqrt{(x_E-\sigma_3)^2 + (y_E - r_2\sin(\theta_0+\theta_2))^2}}\right) - r_2\tan\left[\frac{y_E - r_2\sin\left(\theta_0+\theta_2\right)}{x_E - \sigma_3}\right] \quad (46)$$

$$\sigma_3 = r_2\cos(\theta_0+\theta_2) \quad (47)$$

$$y_M = y_0 - r_{cx}\sin\left(\sigma_1\right) + r_{cy}\sin\left(\frac{\pi}{2} - \sigma_1\right) + \sigma_3 \quad (48)$$

With

$$\sigma_1 = r_2\tan\left(\frac{\sigma_3 - y_E + r_4\sin(\sigma_2)}{x_E - r_2\cos(\theta_0+\theta_2) + r_4\cos(\sigma_2)}\right) \quad (49)$$

$$\sigma_2 = t\cos^{-1}\left(\frac{(x_E - r_2\cos(\theta_0+\theta_2))^2 + (y_E-\sigma_3)^2 - r_3^{\,2} + r_4^{\,2}}{2r_4\sqrt{(x_E - r_2\cos(\theta_0+\theta_2))^2 + (y_E-\sigma_3)^2}}\right) - r_2\tan\left[\frac{y_E - \sigma_3}{x_E - r_2\cos(\theta_0+\theta_2)}\right] \quad (50)$$

$$\sigma_3 = r_2\sin(\theta_0+\theta_2) \quad (51)$$

Coordinates of the coupling point

Let C_x and C_y be the coordinates of the coupling points when the mechanism is in motion. Let $C_x = x_M$ and $C_y = y_M$

We have

$$M = \begin{pmatrix} x_M \\ y_M \end{pmatrix} = \begin{pmatrix} c_x \\ c_y \end{pmatrix} = \begin{pmatrix} x_0 + r_{cy}\cos\left(\frac{\pi}{2} - \sigma_1\right) + \sigma_3 + r_{cx}\cos(\sigma_1) \\ y_0 - r_{cx}\sin\left(\sigma_1\right) + r_{cy}\sin\left(\frac{\pi}{2} - \sigma_1\right) + \sigma_3 \end{pmatrix} \quad (52)$$

C_x and C_y satisfy the equation of the line.

$$y = ax + b \Rightarrow y_M = ax_M + b \quad (53)$$

Table 1. Initial values of projected variables. Point lengths and coordinates are given in [mm] and angles in [rad].

r2	r3	r4	Crx	Cry	X0	Y0	XE	YE	Phi 0	Phi
235	562	607	994	-209	102	-780	384	20	1,2	3,5

Expressions of the objective function and mean error

The problem of synthesizing the four-bar linkage is to minimize the position error considered as the first part of the objective function, which can be expressed.

$$f_{obj} = \sum_{i=1}^{N}\left[\left(C_{Xd}^i - C_X^i(X)\right)^2 + \left(C_{Yd}^i - C_Y^i(X)\right)^2\right] + M_1 h_1(x) + M_2 h_2(x)$$

(54)

$$e_m = \frac{1}{N}\sum_{i=1}^{N}\sqrt{\left(C_{Xd}^i - C_X^i(X)\right)^2 + \left(C_{Yd}^i - C_Y^i(X)\right)^2}$$

(55)

2.1.3 Constraints

$$2\left[\max(r_1,r_2,r_3,r_4) + \min((r_1,r_2,r_3,r_4)\right] \prec (r_1+r_2+r_3+r_4)$$

(56)

$$\theta_2^1 \prec \theta_2^2 \prec \theta_2^3 \prec \ldots \prec \theta_2^N \qquad (57)$$

$$L_i \le x \le u_i \qquad (58)$$

$$\theta_2 \in \left[\frac{\pi}{6};\frac{\pi}{5}\right]$$

$$\min(r_1,r_2,r_3,r_4) = r_2 \qquad (59)$$

If $h_1(x) = 0$ condition (1) is true

If $h_1(x) = 1$ condition (1) is false

If $h_2(x) = 0$ condition (2) is true

If $h_2(x) = 1$ condition (2) is false

M_1 and M_2 are large values that penalize the objective function when the constraints are not verified.

2.2. Diagram of the Mechanism Before Optimizing the Trajectory of Coupling Points

The figure 2 shows the initial 4-bar mechanism as part of a dimensional synthesis with optimization of the objective function.

The crank support point (part connected to the frame) is placed at the beginning of the coordinates x designates the points projected in the case of optimization of the objective function, with curvilinear motion.

- - - the trajectory described by the coupling point before the start of optimization. This figure passes through 16 given points on a straight line.

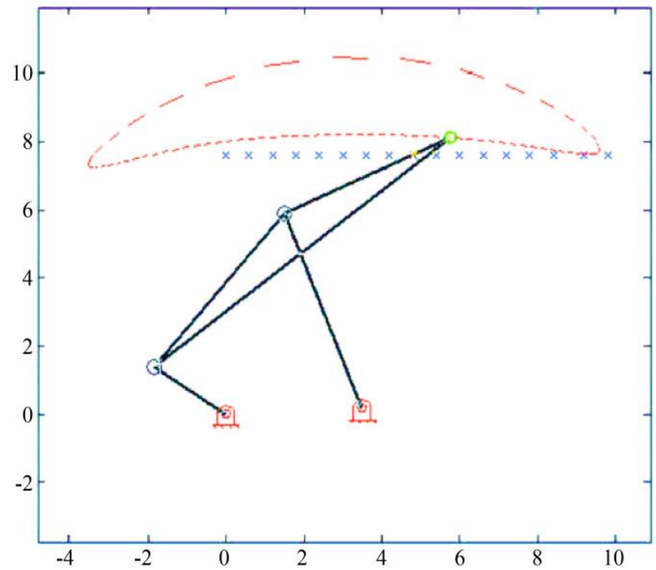

Fig. 2 Diagram of a 4-bar mechanism before optimizing the coupling point trajectory (Radovan R. Bulatovic, Stevan R. Djordjevic, 2004)

The initial values of the variables (mechanism member dimensions and mechanism entry angle) are given in Table 1, with

$$\varphi = \theta_0 + \theta_2 \text{ and } \varphi_1 = \varphi_k - \varphi_0$$

2.3 Diagram of Interactions between Function Blocks Defining Geometrical Relationships in the Mechanism

2.3.1. Function Blocks

Below are some function blocks that can be used to obtain a graph of the function blocks and their interactions.

Freudeinstein Equations Block

```
function [teta_4,teta_3] = fcn(r1,r2,r3,teta_2,r4)
 k1=r1/r2;
k2=r1/r4;
k3=((r2^2-r3^2+r4^2+r1^2)/(2*r2*r4));
k4=r1/r3;
k5=((r4^2-r1^2-r2^2-r3^2)/(2*r2*r3));
G=cos(teta_2-k1-k2*cos(teta_2)+k3);
H=-2*sin(teta_2);
I=k1-(k2+1)*cos(teta_2)+k3;
J=cos(teta_2)-k1+k4*cos(teta_2)+k5;
V=-2*sin(teta_2);
W=k1+(k4-1)*cos(teta_2)+k5;
var1=H.^2-(4*G.*I)/(2*G);
teta_31=2*tan((-V + sqrt(V.^2-(4*J.*W)))/(2*J))^-1;
teta_3=rad2deg(teta_31);
```

```
%teta_4=2*tan((-H + real(sqrt(complex(var1)))))^-1;
teta_4=1;
```

Point A Block

```
function [A,phi] = fcn(teta_2,teta_0,x0,y0,r2)
 % definition of point A
 phi=teta_2+teta_0;
 xa= x0+r2*cos(phi);
ya=y0+r2*sin(phi);
A=[xa;ya];
```

Point B Block

```
function [B,Gphi] = fcn(xe,ye,phi,r2,r4,r3,x0,y0,t,xa,ya)
% definition of point B
ss=sqrt((xe-r2*cos(phi)).^2+(ye-r2*sin(phi)).^2);
teta=r2*tan((ye-r2*sin(phi))/(xe-r2*cos(phi)));
YY=cos((ss.^2+r4^2-r3^2)/(2*ss*r4));
xb=x0+xe+r4*cos(teta-t*YY);
yb=y0+ye+r4*sin(teta-t*YY);
B=[xb;yb];
Gphi=r2*tan((yb-ya)/(xb-xa));
```

Block of point M

```
function M = fcn(x0,y0,r2,phi,Gphi,rcx,rcy)
 % definition of the position of M moving along the trajectory
xm=x0+r2*cos(phi)+rcx*cos(Gphi)+rcy*cos((pi/2)+Gphi);
ym=y0+r2*sin(phi)+rcx*sin(Gphi)+rcy*sin((pi/2)+Gphi);
 M=[xm;ym];
```

Visualization of points A, B, and M

```
function fcn(A,B,M)
figure(4)
x1=A(1,:);
y1=A(2,:);
x2=B(1,:);
y2=B(2,:);
x3=M(1,:);
y3=M(2,:);
subplot(2,2,1);
plot(x1,y1,'-rx', 'MarkerSize', 5);
xlabel('x');
ylabel('y');
title("visualisation point A");
subplot(2,2,2);
plot(x2,y2,'-gx','MarkerSize', 5);
xlabel('x');
ylabel('y');
title("visualisation point B");
subplot(2,1,2);
plot(x3,y3,'-mx','MarkerSize', 5);
%legend('point A', 'point B,"point M','Location', 'northwest');
xlabel('x');
ylabel('y');
title("visualisation point M");
```

After defining all the function blocks resulting from the geometric relations existing in the mechanism, the graph below is generated in Simulink :

When this schematic is generated in SIMULINK, the simulation is launched to observe the different values displayed at the function block outputs and the curves generated by the simulation are visualized.

2.3.2. Interaction Diagram as a Dynamic System

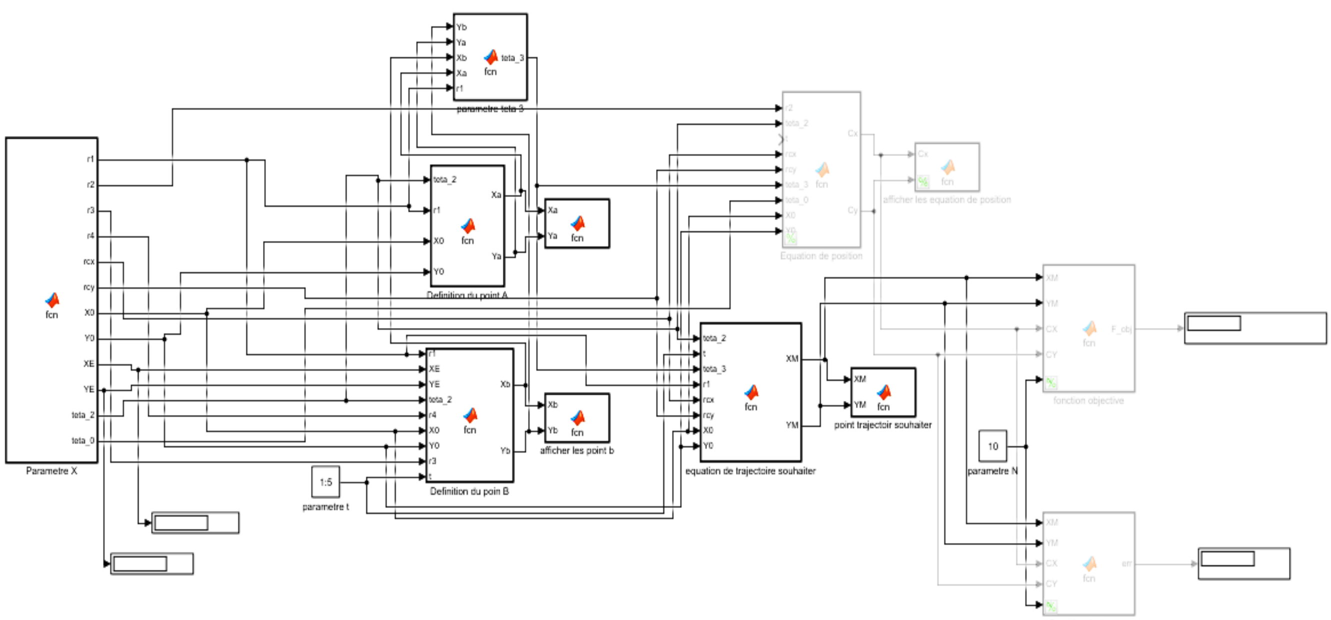

Fig. 3 Interaction diagram as a dynamic system

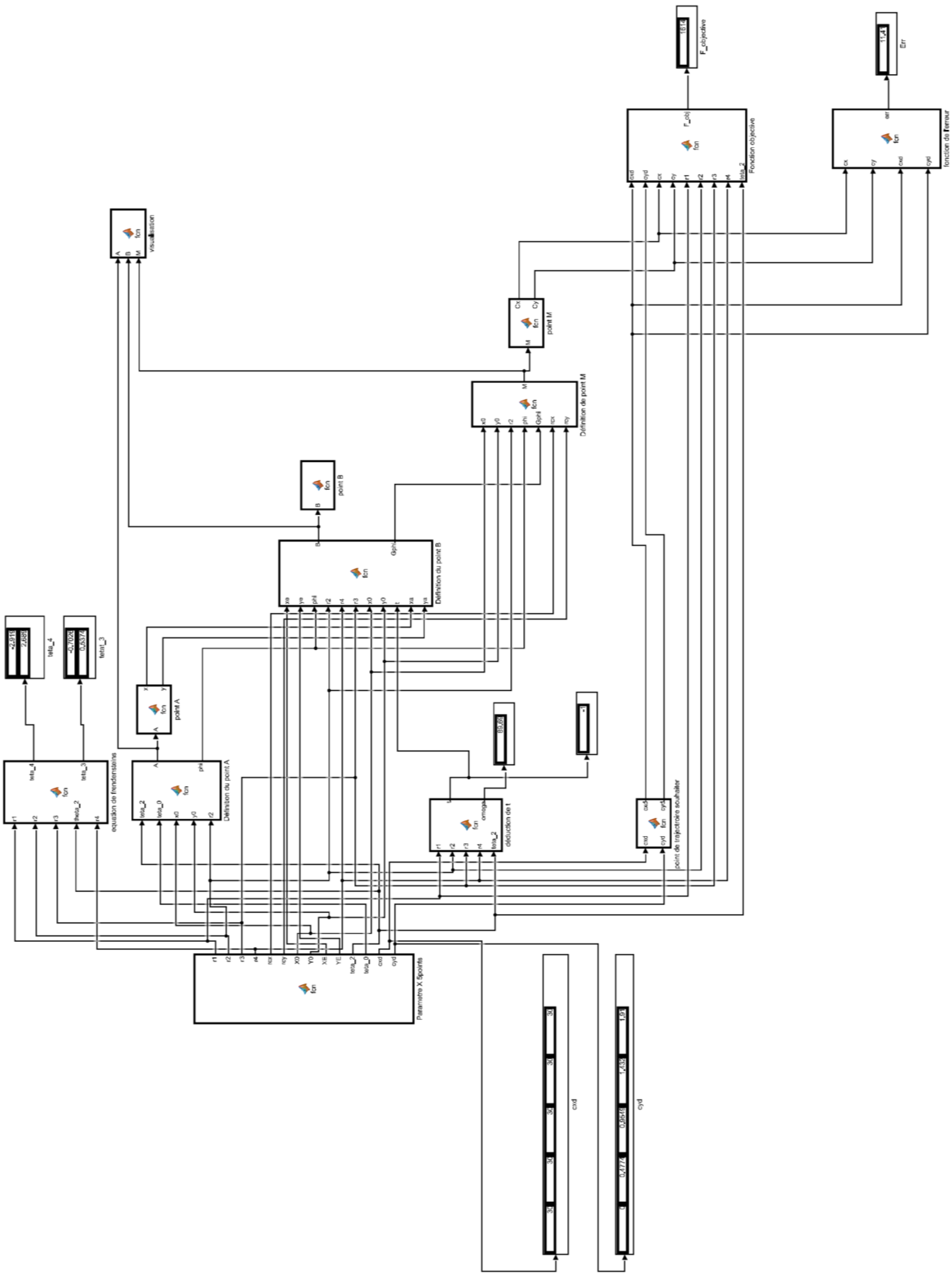

Fig. 4 Function block output values for five precision points

3. Results and Discussion

3.1. Results

3.1.1. Result with Five Points of Precision

Five precision points whose coordinates verify the equation of a straight line are chosen, so the trajectory is a straight line. By analogy, more than five precision points can be taken, and the results should be similar, i.e., a straight trajectory of coupling points should be observed. At the output of the function blocks, values are displayed for dimensional synthesis and visualization of curves showing the trajectories of the mechanism points. values in this graph are entered in tables for greater visibility.

According to the trajectories generated, the precision points and the coupling points are on the same straight line. The trajectory of the coupling point is a vertical straight line. Given that the crank input angle varies in the interval $\left[\frac{\pi}{6};\frac{\pi}{5}\right]$, a rectilinear motion will be observed at the mechanism output.

The figure 4 shows the configuration of the mechanism with five precision points.

Table 2. Precision point coordinates

	P1	P2	P3	P4	P5
X	30	30	30	30	30
Y	0	0,4774	0.9549	1.432	1,91

Table 3. Crank input angle values

θ_2^1	θ_2^2	θ_2^3	θ_2^4	θ_2^5
$\frac{\pi}{6}$	$\frac{21\pi}{120}$	$\frac{11\pi}{60}$	$\frac{23\pi}{120}$	$\frac{\pi}{5}$

Table 4. Coordinate values for different positions of point A

	A1	A2	A3	A4	A5
X	35	35	36,5	39	42,5
Y	22	27	28,5	29,5	29

Table 5. Coordinate values for various positions of point M (Coupling Point)

	M1	M2	M3	M4	M5
X	30	30	30	30	30
Y	0	17	20	21	22

Table 6. Bar distance values and coordinates defining the position of points M and O_2

r1	r2	r3	r4	rcx	rcy	x0	y0
33,5959	5,0297	11,1847	28,0878	24,1755	5,5148	39,7799	24,7195

Table 7. Values of coupler and balance input angles and approximation error

θ_4	θ_3	χ	t	Err	fobj
-2,919	-0,7026	89,69	-1	11,41	1614,06
2,689	0,53				

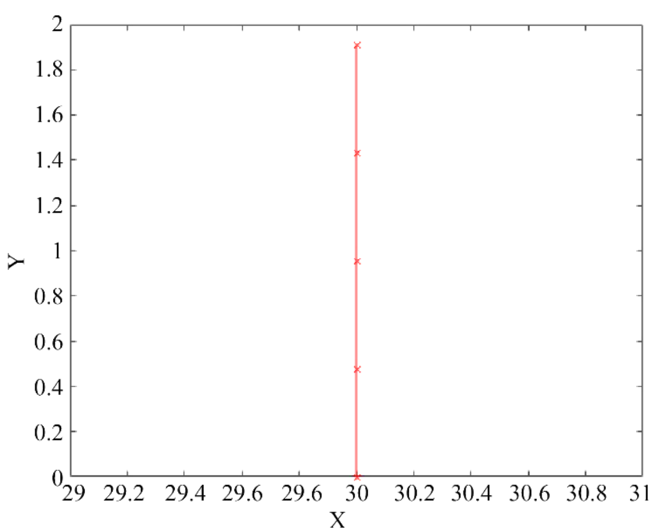

Fig. 5 Right-hand trajectory of precision points

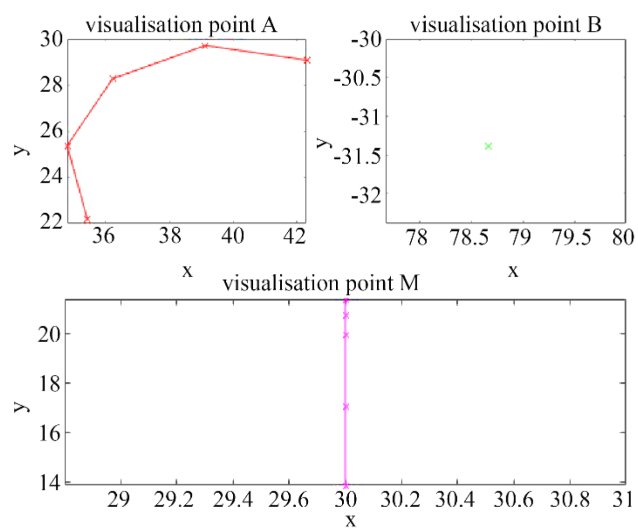

Fig. 6 Trajectory of points A, B and M

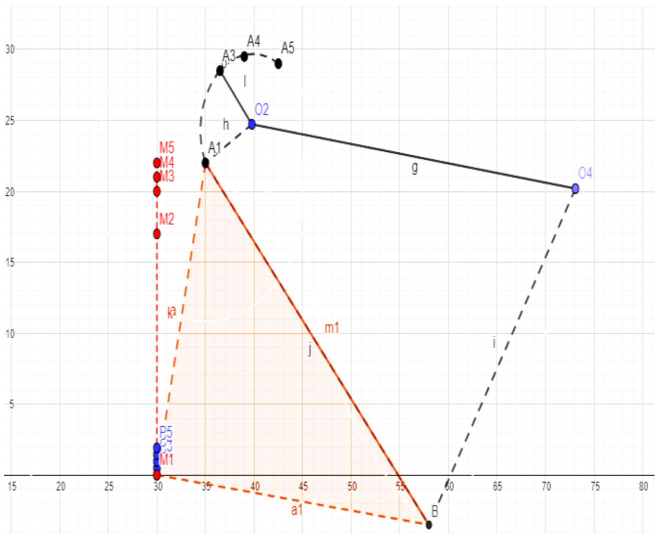

Fig. 7 Straight paths for point M and circular paths for point A When the mechanism is in motion after dimensional synthesis

Comparing the right-hand trajectory observed using this new method with that of the most recent authors working on the dimensional synthesis of 4-bar mechanisms, it emerges that instead of obtaining a curvilinear motion of the coupling point during the operation of the mechanism when the input angle varies by $[0; 2\pi]$, a rectilinear motion is observed in this case, working on a restricted interval $\left[\frac{\pi}{6}; \frac{\pi}{5}\right]$; by constraining the coordinates of the coupling point to verify equation (48)

$$y_M = y_0 - r_{cx}\, sin(\sigma_1) + r_{cy}\, sin\left(\frac{\pi}{2} - \sigma_1\right) + \sigma_3$$

The various trajectories observed after optimization in previous work are shown below.

3.1.2. Results Obtained in Previous Work

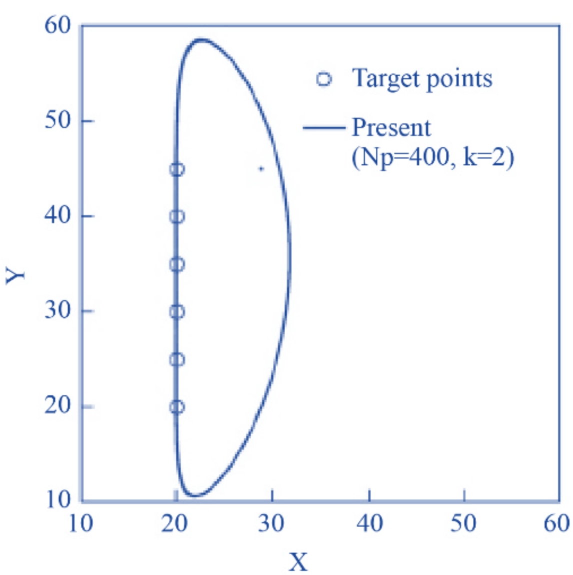

Fig. 8 Curvilinear trajectory of the coupling point (Wen-Yi Lin, 2010)

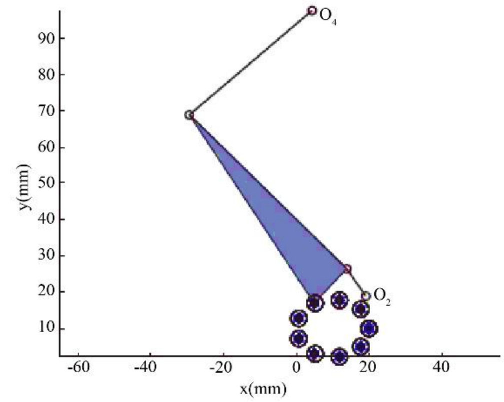

Fig. 9 Curvilinear trajectory of the coupling point after dimensional synthesis (S. Sleesongsom a , S. Bureerat, 2017)

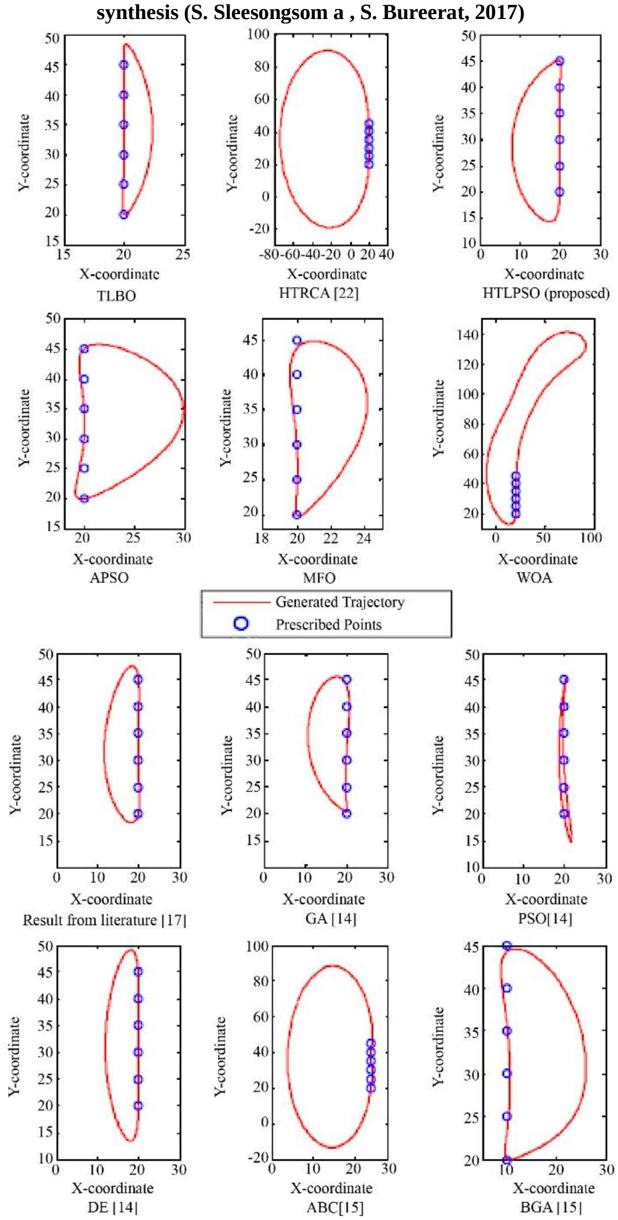

Fig. 10 Coupling point trajectories with dimensional synthesis from genetic algorithms (Ramanpreet Singh, Himanshu Chaudhary and Amit K Singh, 2017).

3.2. Analysis and Discussion

3.2.1. Analytical Programming Analysis

To obtain as many data and parameters as possible for the four-bar mechanism, it is necessary to define it in a global reference frame comprising two reference frames. The first is linked to the frame, and the second is external to the mechanism (reference frame. Thus, as input parameters, it is necessary to mention the coordinates x_0 and y_0 of the fixed point of the frame at the mechanism input (connection point between frame and crank), the lengths of the bars r_1, r_2, r_3, r_4, the coordinates of the coupling point r_{cx}, r_{cy} and the angles θ_0 (angle formed by the frame and the horizontal) and θ_2 (angle formed by the frame and the crank). In fact, in analytical programming, each expression obtained from the existing relationships between distances and angles in the mechanism is given as a function of the input parameters. This makes it possible to track the evolution or displacement of each bar in the mechanism and the coupling point at any given moment.

In this work, the main expressions used to optimize the straight trajectory of a four-bar mechanism are those for s (variable defining the distance between the movable crank vertex and the point E (O_4) on the frame in the reference frame ($O_2X_rY_r$), χ (the angle formed between the coupler and the pendulum); β (the angle formed between the frame and AE), θ_3 (the angle formed between the coupler and the horizontal), θ_4 (the angle formed between the pendulum and the frame), δ (the angle between the crank and the horizontal), A (the center of the connection between the crank and the coupler), B (the center of the connection between the coupler and the pendulum), E (the center of the connection between the frame and the pendulum). Analytical programming on Matlab enables us to obtain these different expressions exclusively as a function of the input parameters.

3.2.2. Analysis of Graphical Programming as a Dynamic System on Simulink

After obtaining the various expressions in the 4-bar mechanism as a function of the input parameters, the various data for the vector of design variables X, the Freudeinstein equations, the point M describing the desired trajectory, points A, B, the objective function, the mean error, etc., are introduced into the Simulink part in the form of function blocks. Subsequently, all the interactions and relationships or links between these data are highlighted, so the whole is treated as a dynamic system where the points evolve over time.

Depending on the number of precision points and the input data on bar lengths, simulations are carried out for each case. The results are displayed in function block graphs with the values sought as outputs and in graphical form with the trajectories of points A, B, and M. This can be seen in Figures 4, 5, and 6.

3.2.3. Analysis and Interpretation of Results

It should be noted that prior to optimization of the coupling point trajectory (Figure 2), the latter is curvilinear, as seen in the most recent previous work. [9,10]

They aim to bring the pre-optimization points as close as possible to the desired post-optimization points. The results of this work show that if the input angle varies between,

$$\left[\frac{\pi}{6};\frac{\pi}{5}\right]$$

then the trajectory is rectilinear; by forcing the coupling point to describe the equation of a straight line, it emerges that for five points of precision, the trajectory is a Tables 2 and 3 show that for each value of the target points, there is a corresponding value of the entry angle between the frame and the crank. When the crank makes a complete turn, i.e., varies between [0;2π], the trajectory of the coupling point is curvilinear. [9,10]

On the other hand, when this interval is subdivided, the trajectory becomes closer to a straight line. After several iterations, it appears that it is in the interval $\left[\frac{\pi}{6};\frac{\pi}{5}\right]$ that the trajectory is a straight line. In previous works. [10,11,12,13,14,15,16,17,18,19,20,21,22,23,24,25,26,27,28,29,30]The authors focused solely on the dimensional synthesis of for-bar mechanisms using various objective function optimization methods (GA, PSO, DE, ABC, BGA, HTRCA APSO, MFO, HTLPSO, WOA), as shown in Figures 8, 9, and 10, to minimize the error between the trajectory of the target points and that of the coupling points. As a result, at the end of their study, point M describes a curvilinear trajectory. With this method, the trajectory of the coupling point is imposed during the analytical programming; its coordinates are constrained to verify the equations of the line

$$y = y_0 - r_{cx}\sin(\sigma_1) + r_{cy}\sin\left(\frac{\pi}{2}-\sigma_1\right) + \sigma_3$$

and

$$x = x_0 + r_{cy}\cos\left(\frac{\pi}{2}-\sigma_1\right) + \sigma_3 + r_{cx}\cos(\sigma_1)$$

; through which the target points also pass.

Similarly, to ensure that only rectilinear movement of the mechanism is obtained, the input angle sweep interval is reduced to $\left[\frac{\pi}{6};\frac{\pi}{5}\right]$; this can be controlled by a servomotor at the input. The end result is a four-bar mechanism that performs a rectilinear reciprocating movement in this interval.

After simulation on Simulink, Figure 6 shows the successive positions occupied by points A, B, and M with 5 accuracy points. The values of bar length, some coordinates, angles, errors, and objective functions are also shown (Tables 6 and 7).

The latter's values are high, implying that the method developed here cannot be optimized. Here, the sum of the distances of the smallest and largest bars (r2+r1) is less than the sum of the distances of the other two bars (r3+r4), so the Grashoff condition is satisfied; r2 is the crank and can perform a full rotation. This justifies the circular trajectory of point A. It follows that the configuration of this mechanism is that of a Crank-Balance WheelFigures 5 and 6 show that the precision and coupling points pass through the same straight line, confirming the straight trajectory at the exit.

4. Conclusion

In summary, this study aimed to provide a dimensional synthesis of four-bar mechanisms for generating rectilinear motion through analytical and graphical programming and to optimize the straight trajectory of the coupling point. Analytical and graphical programming enables us to treat the problem by subdividing it into function program blocks and highlighting the interactions between them in the form of a dynamic system. Optimization of the trajectory is achieved by forcing the coupling point to pass only on a straight line, thus obtaining rectilinear motion instead of a curvilinear curve, as encountered in the literature.

5. Perspective

When optimizing the right-hand trajectory of the coupling point, the value of the mean error associated with that of the objective function is not optimal. It would be advisable to exploit the results obtained to optimize the objective function with linear or nonlinear programming and then compare the results with those obtained with genetic algorithms or hybridize the algorithms to obtain optimal values. The case of rectilinear motion has been dealt with for four-bar mechanisms. The study will be extended to six-bar mechanisms, using the Hart model, and to eight-bar mechanisms, using the Peaucelier-Lipkin model for dimensional synthesis, and finally, working on their stability during operation.

Acknowledgments

Thanks to all those who contributed to the success of this work. All authors contributed to the study's conception and design, material preparation, data collection, programming, simulation, validation, and analysis.

References

[1] George N. Sandor, "*A General Complex Number Method for Plane Kinematic Synthesis with Application*," Columbia University, New York, pp. 1-24, 1959. [Google Scholar] [Publisher Link]

[2] Arthur G. Erdman, and George N. Sandor, *Advanced Mechanism Design: Analysis and Synthesis*, Prentice-Hall, Upper Saddle River, NJ, vol. 2, pp. 1-688, 1984. [Google Scholar] [Publisher Link]

[3] A.P. Morgan, and C.W. Wampler, "Solving a Planar Four-Bar Design Problem Using Continuation," *Journal of Mechanical Design*, vol. 112, no. 4, pp. 544-550, 1990. [CrossRef] [Google Scholar] [Publisher Link]

[4] Han Chi-Yeh, "A General Method for the Optimum Design of Mechanisms," *Journal of Mechanisms*, vol. 1, no. 3-4, pp. 301-313, 1966. [CrossRef] [Google Scholar] [Publisher Link]

[5] S. Krishnamurty, and David A. Turcic, "Optimal Synthesis of Mechanisms Using Nonlinear Goal Programming Techniques," *Mechanisms and Machine Theory*, vol. 27, no. 5, pp. 599-612, 1992. [CrossRef] [Google Scholar] [Publisher Link]

[6] Jawaharlal Mariappan, and Sundar Krishnamurty, "A Generalized Exact Gradient Method for Mechanism Synthesis," *Mechanism and Machine Theory*, vol. 31, no. 4, pp. 413-421, 1996. [CrossRef] [Google Scholar] [Publisher Link]

[7] Yu Hongying, Tang Dewei, and Wang Zhixing, "Study on a New Computer Path Synthesis Method of a Four-Bar Linkage," *Mechanism and Machine Theory*, vol. 42, no. 4, pp. 383-392, 2007. [CrossRef] [Google Scholar] [Publisher Link]

[8] Jacek Buśkiewicz, Roman Starosta, and Tomasz Walczak, "On the Application of the Curve Curvature in Path Synthesis," *Mechanism and Machine Theory*, vol. 44, no. 6, pp. 1223-1239, 2009. [CrossRef] [Google Scholar] [Publisher Link]

[9] Radovan R. Bulatovic, and Stevan R. Djordjevic, "Optimal Synthesis of a Four-Bar Linkage by Method of Controlled Deviation," *Theoretical and Applied Mechanics*, vol. 31, no. 3-4, pp. 265-280, 2004. [CrossRef] [Google Scholar] [Publisher Link]

[10] Wen-Yi Lin, "A GA–DE Hybrid Evolutionary Algorithm for Path Synthesis of Four-Bar Linkage," *Mechanism and Machine Theory*, vol. 45, no. 8, pp. 1096-1107, 2010. [CrossRef] [Google Scholar] [Publisher Link]

[11] S. Sleesongsom, and S. Bureerat, "Four-Bar Linkage Path Generation through Self-Adaptive Population Size Teaching-Learning Based Optimization," *Knowledge-Based Systems*, vol. 135, pp. 180-191, 2017. [CrossRef] [Google Scholar] [Publisher Link]

[12] S.K. Acharyya, and M. Mandal, "Performance of EAs for Four-Bar Linkage Synthesis," *Mechanism and Machine Theory*, vol. 44, no. 9, pp. 1784-1794, 2009. [CrossRef] [Google Scholar] [Publisher Link]

[13] J.A. Cabrera, A. Simon, and M. Prado, "Optimal Synthesis of Mechanisms with Genetic Algorithms," *Mechanism and Machine Theory*, vol. 37, no. 10, pp. 1165-1177, 2002. [CrossRef] [Google Scholar] [Publisher Link]

[14] Xiong Zhang, Ji Zhou, and Yingyu Ye, "Optimal Mechanism Design Using Interior-Point Methods," *Mechanism and Machine Theory*, vol. 35, no. 1, pp. 83-98, 2000. [CrossRef] [Google Scholar] [Publisher Link]

[15] R. Sancibrian et al., "A General Procedure based on Exact Gradient Determination in Dimensional Synthesis of Planar Mechanisms,"

Mechanism and Machine Theory, vol. 41, no. 2, pp. 212-229, 2006. [CrossRef] [Google Scholar] [Publisher Link]

[16] Seyedali Mirjalili, and Andrew Lewis, "The Whale Optimization Algorithm," *Advances in Engineering Software*, vol. 95, pp. 51-67, 2016. [CrossRef] [Google Scholar] [Publisher Link]

[17] Seyedali Mirjalili, "Moth-Flame Optimization Algorithm: A Novel Nature-Inspired Heuristic Paradigm," *Knowledge-Based Systems*, vol. 89, pp. 228-249, 2015. [CrossRef] [Google Scholar] [Publisher Link]

[18] Horacio Martínez-Alfaro, *Four-Bar Mechanism Synthesis for n Desired Path Points Using Simulated Annealing*, Advances in Metaheuristics for Hard Optimization, Springer Berlin, pp. 23-27, 2007. [CrossRef] [Google Scholar] [Publisher Link]

[19] R.V. Rao, V.J. Savsani, and D.P. Vakharia, "Teaching–Learning-Based Optimization: A Novel Method for Constrained Mechanical Design Optimization Problems," *Computer-Aided Design*, vol. 43, no. 3, pp. 303-315, 2011. [CrossRef] [Google Scholar] [Publisher Link]

[20] Xinsheng Lai, and Mingyi Zhang, "An Efficient Ensemble of GA and PSO for Real Function Optimization," *Proceedings of the 2nd IEEE International Conference on Computer Science and Information Technology*, ICCSIT, Beijing, pp. 651-655, 2009. [CrossRef] [Google Scholar] [Publisher Link]

[21] Jong-Won Kim et al., "Numerical Hybrid Taguchi-Random Coordinate Search Algorithm for Path Synthesis," *Mechanism and Machine Theory*, vol. 102, pp. 203-216, 2016. [CrossRef] [Google Scholar] [Publisher Link]

[22] Hamed Soleimani, and Govindan Kannan, "A Hybrid Particle Swarm Optimization and Genetic Algorithm for Closed-Loop Supply Chain Network Design in Large-Scale Networks," *Applied Mathematical Modelling*, vol. 39, no. 14, pp. 3990-4012, 2015. [CrossRef] [Google Scholar] [Publisher Link]

[23] C.K. Yogesh et al., "A New Hybrid PSO Assisted Biogeography-Based Optimization for Emotion and Stress Recognition from Speech Signal," *Expert Systems with Applications*, vol. 69, pp. 149-158, 2017. [CrossRef] [Google Scholar] [Publisher Link]

[24] Arijit De et al., "Composite Particle Algorithm for Sustainable Integrated Dynamic Ship Routing and Scheduling Optimization," *Computers & Industrial Engineering*, vol. 96, pp. 201-215, 2016. [CrossRef] [Google Scholar] [Publisher Link]

[25] Arijit De, Anjali Awasthi, and Manoj Kumar Tiwari, "Robust Formulation for Optimizing Sustainable Ship Routing and Scheduling Problem," *IFAC-PapersOnLine*, vol. 48, no. 3, pp. 368-373, 2015. [CrossRef] [Google Scholar] [Publisher Link]

[26] Arijit De et al., "Sustainable Maritime Inventory Routing Problem with Time Window Constraints," *Engineering Applications of Artificial Intelligence*, vol. 61, pp. 77-95, 2017. [CrossRef] [Google Scholar] [Publisher Link]

[27] Vimal Kumar Pathak et al., "A Modified Algorithm of Particle Swarm Optimization for form Error Evaluation," *Technisches Messen*, vol. 84, no. 4, pp. 272-292, 2017. [CrossRef] [Google Scholar] [Publisher Link]

[28] Suraya Masrom et al., "Hybridization of Particle Swarm Optimization with Adaptive Genetic Algorithm Operators," *Proceedings of the 13th IEEE International Conference on Intelligent Systems Design and Applications*, Salangor, Malaysia, pp. 153-158, 2013. [CrossRef] [Google Scholar] [Publisher Link]

[29] Dipankar Santra et al., "Hybrid PSO–ACO Algorithm to Solve Economic Load Dispatch Problem with Transmission Loss for Small Scale Power System," *Proceedings of the 2016 International Conference on Intelligent Control Power and Instrumentation*, Kolkata, India, pp. 226-230, 2016. [CrossRef] [Google Scholar] [Publisher Link]

[30] Alex Alexandridis, Eva Chondrodima, and Haralambos Sarimveis, "Cooperative Learning for Radial Basis Function Networks Using Particle Swarm Optimization," *Applied Soft Computing*, vol. 49, pp. 485-497, 2016. [CrossRef] [Google Scholar] [Publisher Link]